DR2003071

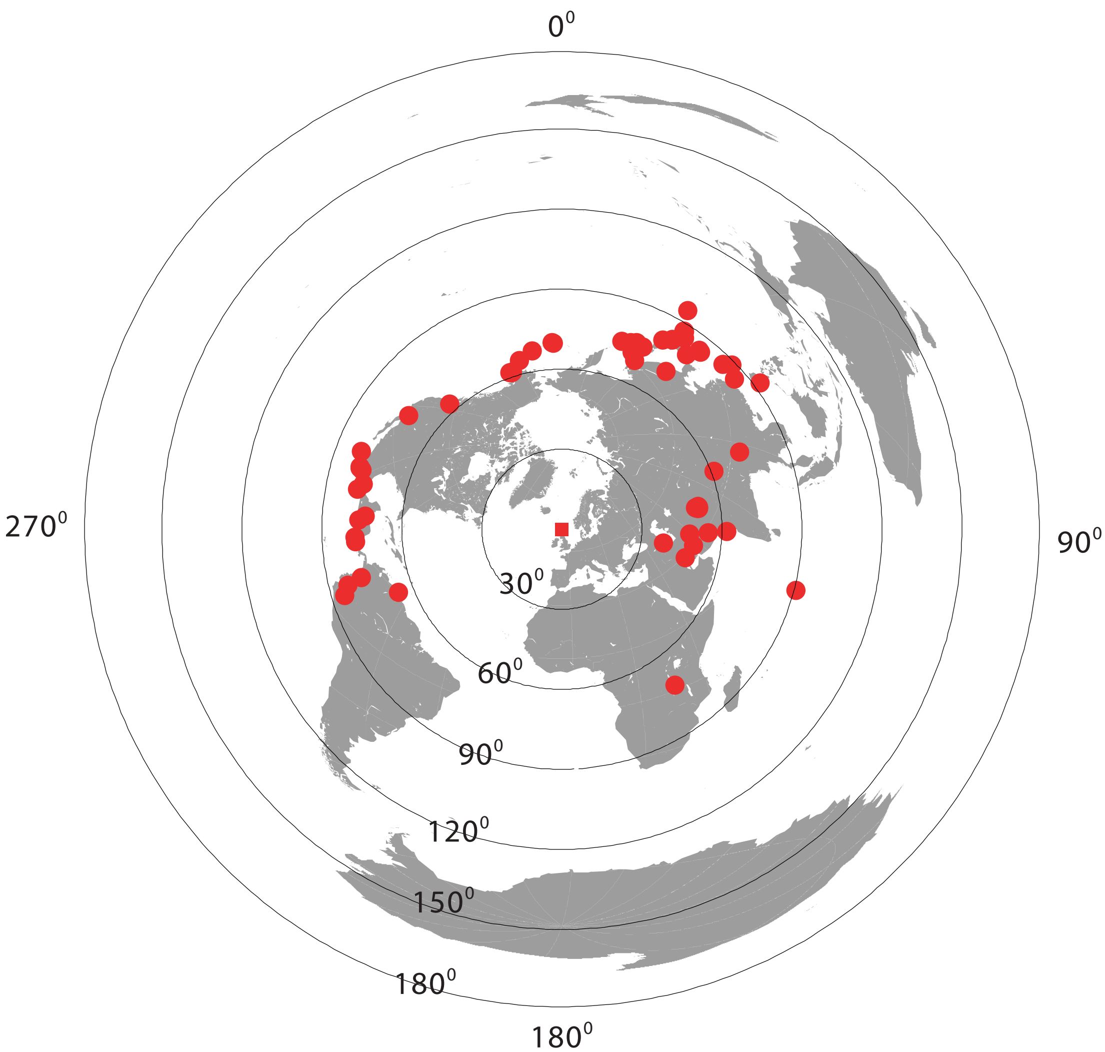

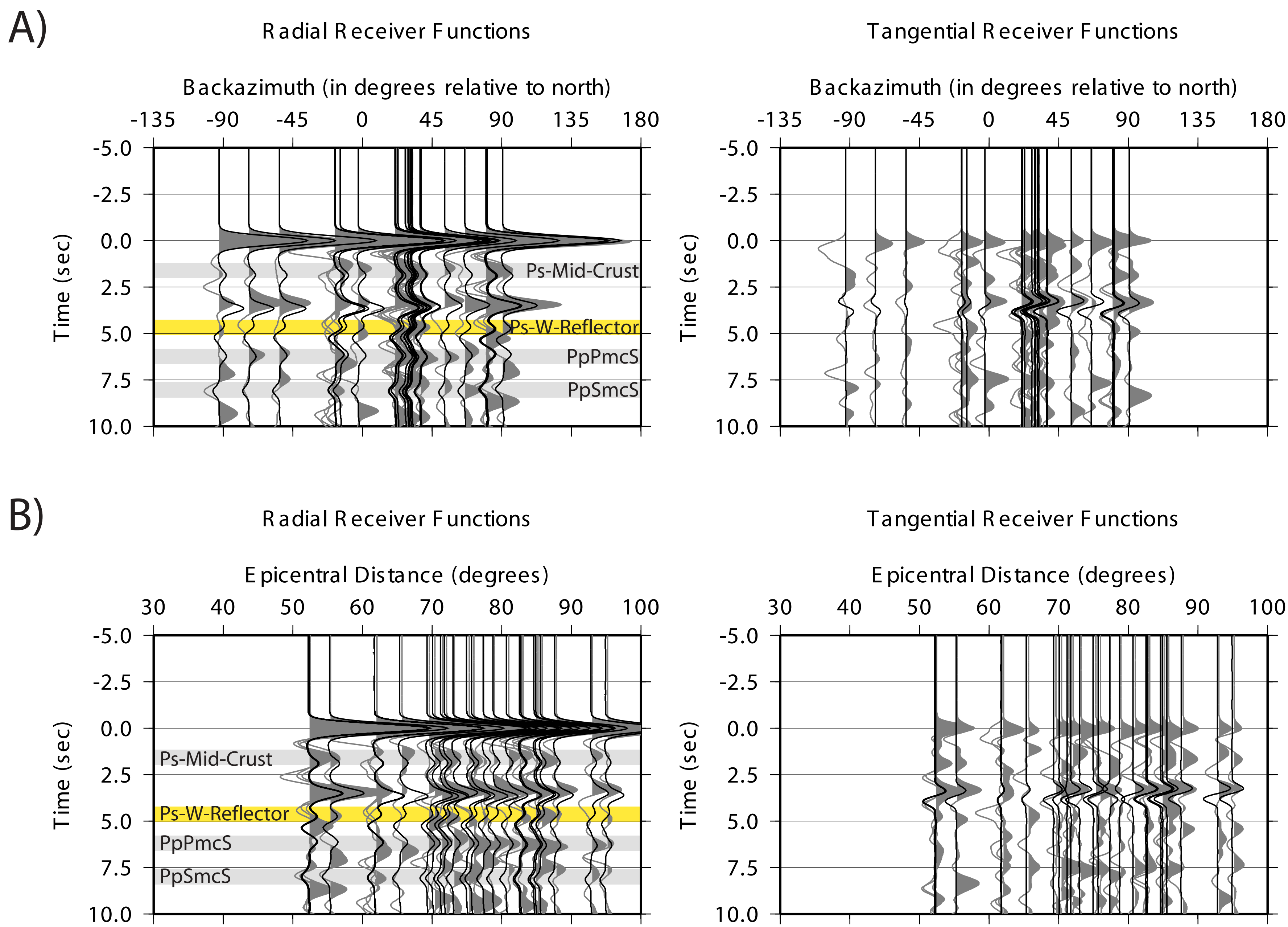
A)
Radial Receiver Functions
Backazimuth (in degrees relative to north)
-135 -90 -45 0 45 90 135 180
-5.0 -2.5 0.0 2.5 5.0 7.5 10.0
Time (sec)
Ps-Mid-Crust
Ps-W-Reflector
PpPmcS
PpSmcS
Tangential Receiver Functions
Backazimuth (in degrees relative to north)
B)
Radial Receiver Functions
Epicentral Distance (degrees)
30 40 50 60 70 80 90 100
Ps-Mid-Crust
Ps-W-Reflector
PpPmcS
PpSmcS
Tangential Receiver Functions
Epicentral Distance (degrees)

GSA Data Repository Item

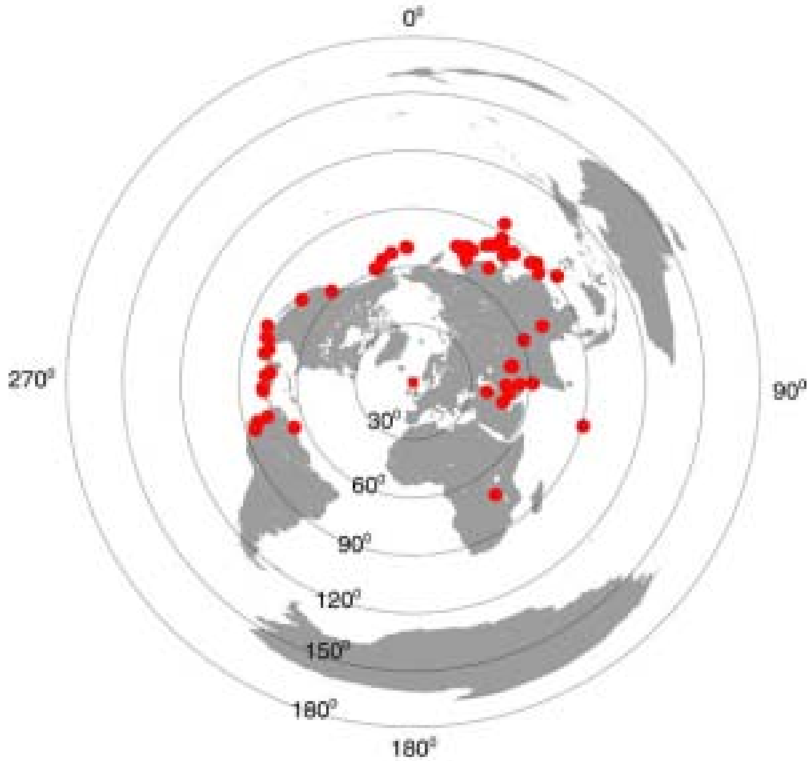

Figure DR1. Global seismicity distribution relative to North Scotland used in this study. Most of the events originated from the north-east, east and west, with no event back azimuth coverage from the south or south-east. A total of 65 events (M>6.0; Table DR2) occurring between epicentral distances of 30^o to 90^o from the stations were processed to obtain receiver functions using the iterative time-domain deconvolution method of Ligorría and Ammon (1999). The iterative time-domain deconvolution method is a least-squares minimization approach of the difference between the observed horizontal seismogram and a predicted signal generated by the convolution of an iteratively updated spike train with the vertical component seismogram. Events that reproduce 80% or greater of the observed power of the horizontal seismogram (convolve the radial receiver function and the vertical seismogram to match the radial seismogram) were retained for this analysis. To removed long-period noise before calculating receiver functions we filtered the original broadband (BACA) seismograms with two passes of a high-pass, two-pole butterworth filter with corner frequencies at 0.7 Hz. Each individual event recorded by the elements of the broadband array (BACA) was stacked to improve signal-to-noise ratio. A 0.33 s gaussian low pass filter was used to remove high-frequency noise.

GSA Data Repository Item

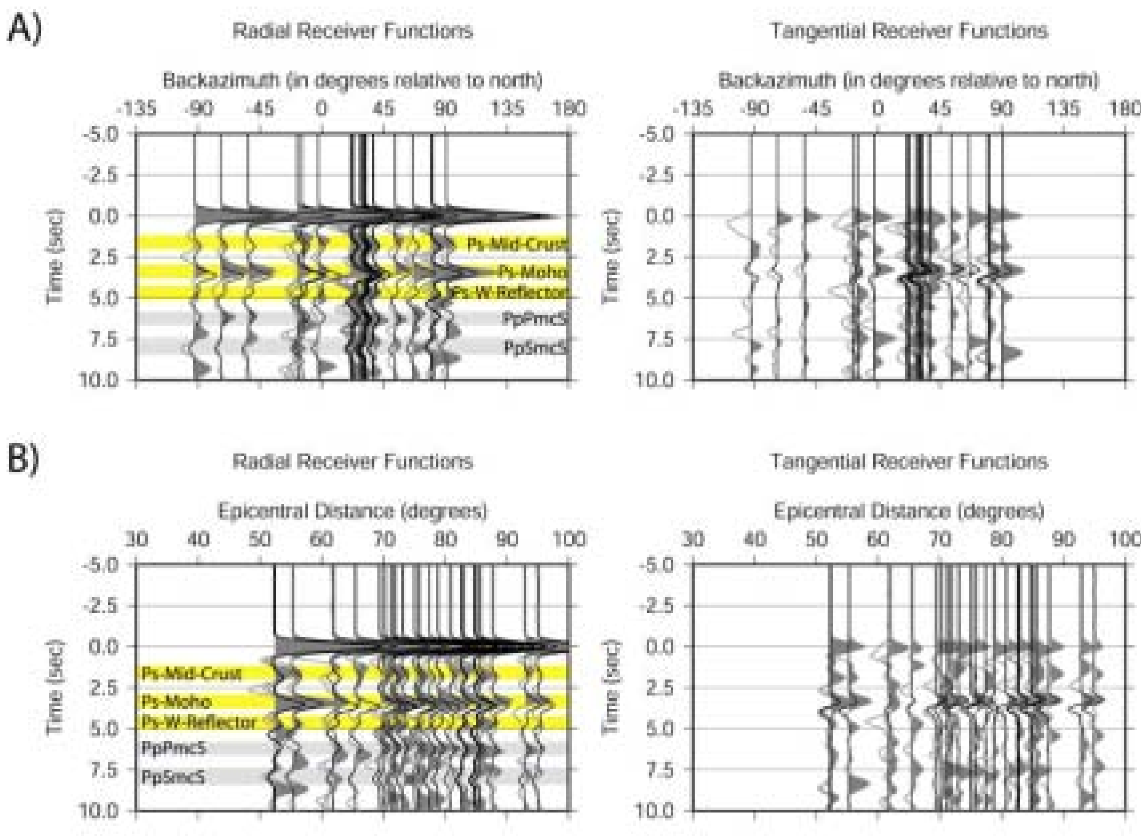

Figure DR2. BACA observed and modeled radial and Tangential receiver functions plotted A) against backazimuth and B) against epicentral distance. All waveforms shown are individual receiver functions. Highlighted (in yellow) are *Ps* conversions from the Mid-Crust (~1.5 s), Moho (~3.1 s) and the W-Reflector (~5.0 s). Multiples from the Mid-Crust (*PpPmcS* and *PpPmcS*) are highlighted in gray. *PpPmcS* refers to a *P*-wave reflected once from the free surface and then converted to a shear wave upon reflection from the Mid-Crust. Similarly, *PpSmcS* refers to a *P*-wave reflected once as *S*-wave and then converted to a shear wave upon reflection from the Mid-Crust. *Ps* phase arrival from the W-Reflector are clear only for events arriving from the N-NE and very weak from the west and east.

Table DR1. Seismometer Coordinates And Operation Period (Broadband Stations).

Station	Latitude	Longitude	Sensor Type	Operation Period (Year/Julian Date)
BANN	58.5221	-4.2113	Guralp CMG-3T	1999/270-2000/258
BAWA	58.5025	-4.2173	Guralp CMG-3T	1999/273-2000/257
BASS	58.4821	-4.1991	Guralp CMG-3T	1999/271-2000/259
BABE	58.5133	-4.1500	Guralp CMG-3T	1999/278-2000/256
BACA	58.5015	-4.2026	Guralp CMG-3T	1999/274-2000/259
ORE	58.5480	-3.7622	Willmore MK -III	UKSN
RRR	57.8577	-5.8067	Willmore MK -III	UKSN

Note: A five-seismometer (BANN, BAWA, BASS, BABE and BACA), star shaped array with ~ 2-km station spacing ("fat station") was installed at Bettyhill, northern Scotland. Center station BACA was used as our reference station. The fat station approach was designed to enhance teleseismic signal relative to noise and reduce scattering in subsequent receiver functions calculations. Events gathered through the British Geological Survey Autodrm Database system from January 1997 through September 2001 complement our data set.

Table DR2. List Of Events

Event	Time, UT	Latitude	Longitude		Stations						
					BANN	BAWA	BASS	BABE	BACA	ORE	RRR
1997.011	20:28:28.00	18.173	102.834	49.30							X
1997.121	11:37:34.20	18.995	107.267	15.00							X
1997.130	07:57:29.60	33.878	59.823	6.70						X	X
1997.133	14:13:46.20	36.482	71.000	198.10						X	X
1997.142	07:50:55.30	18.671	101.658	84.60							X
1997.168	21:03:40.50	51.314	179.315	33.00						X	X
1997.190	19:24:10.20	10.505	-63.545	3.00						X	X
1997.195	16:09:31.40	43.163	146.430	6.90						X	
1997.225	04:45:03.20	25.132	125.867	39.50						X	
1997.245	12:13:23.10	3.879	-75.698	196.40						X	X
1997.301	06:15:19.20	-4.351	-76.675	127.50						X	X
1997.312	10:02:53.40	35.116	87.374	0.00						X	X
1998.051	12:18:06.20	36.479	71.086	235.60						X	
1998.073	19:40:27.00	30.154	57.605	9.00						X	X
1998.080	18:22:28.50	36.433	70.133	227.80						X	
1998.093	22:01:48.20	-8.148	74.238	164.60						X	X
1998.123	23:30:21.90	22.306	125.308	33.00						X	X
1998.150	06:22:29.00	37.106	70.110	33.00						X	X

Table DR2. List Of Events (cont.)

	Time, UT	Latitude	Longitude		Stations						
					BANN	BAWA	BASS	BABE	BACA	ORE	RRR
1998.190	14:19:18.40	38.717	48.507	26.00						X	X
1998.232	06:40:55.80	28.932	139.329	440.50						X	X
1999.028	08:10:05.40	52.886	169.123	67.20						X	
1999.098	13:10:34.10	43.607	130.350	565.70						X	X
1999.126	23:00:53.10	29.501	51.880	33.00						X	
1999.128	19:44:36.00	45.449	151.630	62.70						X	
1999.132	17:59:22.40	43.032	143.835	102.70							X
1999.166	20:42:05.90	18.386	-97.436	70.00						X	X
1999.192	14:14:16.50	15.782	-88.330	10.00						X	X
1999.232	10:02:21.10	9.044	-84.159	20.00						X	X
1999.240	12:40:06.20	-1.287	-77.549	196.40							X
1999.263	17:47:18.50	23.772	120.982	33.00							X
1999.273	16:31:15.70	16.059	-96.931	60.60						X	X
1999.286	01:33:40.10	54.657	161.189	30.00	X	X	X	X	X		
1999.289	09:46:44.10	34.594	116.271	0.00	X	X	X	X	X	X	X
1999.312	16:45:43.00	36.522	71.240	228.40	X	X	X	X	X	X	X
1999.340	23:12:33.90	57.413	154.489	66.00	X	X	X	X	X		X
1999.341	00:19:49.60	57.362	154.514	40.90	X	X	X	X	X		
1999.345	18:03:36.50	15.766	119.740	33.00	X	X	X	X	X		
2000.028	14:21:07.30	43.046	146.837	61.10			X		X	X	X
2000.088	11:00:22.50	22.338	143.730	126.50	X	X	X		X		X
2000.133	23:10:30.00	35.975	70.657	107.70	X	X	X				X
2000.156	17:52:16.00	28.723	65.383	33.00	X	X	X				
2000.158	14:57:02.20	29.424	131.421	33.00	X	X	X			X	
2000.159	21:46:55.90	26.856	97.238	33.00	X	X	X				X
2000.161	23:31:45.30	30.491	137.730	485.30	X	X	X				
2000.167	11:10:46.20	29.368	132.082	10.00	X	X	X				
2000.189	15:46:44.60	51.411	179.978	31.00	X	X	X				X
2000.190	18:57:44.50	34.053	139.126	10.00	X	X	X				
2000.192	09:58:19.00	46.828	145.422	359.60	X	X	X				
2000.193	01:32:28.50	57.369	154.206	43.60	X	X	X			X	X
2000.199	22:53:47.30	36.283	70.924	141.40	X	X	X			X	X
2000.202	18:39:18.80	36.510	140.983	47.10	X	X	X			X	
2000.203	01:53:35.80	9.416	-85.329	33.00	X	X	X				X
2000.212	12:25:45.60	33.901	139.376	10.00	X	X	X			X	
2000.217	21:13:02.70	48.786	142.246	10.00	X	X	X			X	X
2000.219	07:27:12.90	28.856	139.556	394.80	X	X	X			X	X
2000.222	11:41:47.90	18.198	102.480	45.80	X	X	X				
2000.232	17:26:27.90	43.816	147.167	62.40	X	X	X				
2000.276	02:25:31.30	-7.977	30.709	34.00							X
2001.010	16:02:44.20	57.078	153.211	33.00						X	X
2001.013	17:33:32.40	13.049	-88.660	60.00						X	X
2001.026	03:16:40.50	23.419	70.232	16.00						X	X
2001.056	02:21:59.60	36.424	70.881	202.50						X	
2001.059	18:54:32.80	47.149	122.727	51.90							X
2001.083	06:27:53.60	34.083	132.526	50.00						X	
2001.145	00:40:50.60	44.268	148.393	33.00						X	

Table DR3. Average Crustal Thickness And Vp/Vs Ratios

Station	Depth	Vp/Vs Ratio

	(km)	
ORE	26.1 ± 1.1	1.74 ± 0.06
BACA	27.5 ± 0.9	1.75 ± 0.05
RRR	23.8 ± 1.2	1.79 ± 0.09

Note: We used the technique outlined by Zhu and Kanamori (2000), a stacking algorithm which sums the amplitudes of receiver functions at the predicted times of the Moho *Ps* converted phase and the later multiple (*PpPms* and *PpSms*+*PsPms*) converted phases, by different crustal thickness and V_p/V_s ratios. This transforms the time domain receiver functions directly into the Depth (H)-V_p/V_s domain without need to identify these phases and to pick their arrival times (Zhu and Kanamori, 2000). The best estimation of the crustal thickness and V_p/V_s ratio are found when the three phases stack coherently.

Table DR4. ORE Velocity Model

Layer	V_p (km/s)	V_s (km/s)	□ (kg/m^3)	Z (km)
1	6.20	3.56	2754	7.0
2	6.40	3.66	2808	10.4
3	6.60	3.79	2890	8.9
4	8.10	4.67	3362	21.7
5	8.50	4.91	3490	10.0
6	8.10	4.67	3362	-

Note: Only layer 5 was modeled as an anisotropic interface. The anisotropy is parametrized as a 10% percentage variation in P- and S-wave velocity. Tilt axis =90^o (horizontal); Symmetry axis azimuth=N57^{o}E . See Frederiksen and Bostock (2000) for details of parameter definition.

GSA Data Repository Item

Table DR5. RRR Velocity Model

Layer	V_p (km/s)	V_s (km/s)	□ (kg/m^3)	Z (km)
1	6.10	3.41	2722	9.0
2	6.46	3.61	2837	15.0
3	8.10	4.67	3362	15.0

4	8.50	4.91	3490	5.0
5	8.10	4.67	3362	-

Note: Only layer 4 was modeled as an anisotropic interface. The anisotropy is parametrized as a 15% percentage variation in P- and S-wave velocity. Tilt axis =90^{o} (horizontal); Symmetry axis azimuth=N143^{o}E . See Frederiksen and Bostock (2000) for details of parameter definition.

Table DR6. BACA Velocity Model

Layer	V_p (km/s)	V_s (km/s)	□ (kg/m^3)	Z (km)
1	6.20	3.54	2754	7.0
2	6.40	3.50	2808	7.5
3	6.60	3.77	2890	13.0
4	8.10	4.67	3362	4.0
5	8.10	4.67	3362	10.0
6	8.50	4.91	3490	5.0
7	8.10	4.67	3362	-

Note: Only layer 4 was modeled as an anisotropic interface. The anisotropy is parametrized as a 10% percentage variation in P- and S-wave velocity. Tilt axis =75^{o}; Symmetry axis azimuth=N136^{o}E . See Frederiksen and Bostock (2000) for details of parameter definition.

2003071 Asencio et al, 2003

~~GSA Data Repository Item~~

References Cited in Figures and Tables

Frederiksen, A.W., and Bostock, M.G., 2000, Modelling teleseismic waves in dipping anisotropic structures: Geophysical Journal International, v. 141, p. 401-412.

Ligorría, J.P., and Ammon, C.J., 1999, Iterative Deconvolution and Receiver-Function Estimation: Bulletin of the Seismological Society of America, v. 89, p. 1395-1400.

Zhu, L., and Kanamori, H., 2000, Moho depth variation in Southern California from teleseismic receiver functions: Journal of Geophysical Research, B, Solid Earth and Planets, v. 105, p. 2969-2980.